ELSEVIER

Earth and Planetary Science Letters 206 (2003) 215–228

EPSL

www.elsevier.com/locate/epsl

Magnetic fabrics from the Costa Rica margin: sediment deformation during the initial dewatering and underplating process

Bernard A. Housen [a,*], Toshiya Kanamatsu [b]

[a] *Pacific NW Paleomagnetism Laboratory, Geology Department, Western Washington University, 516 High Street, Bellingham, WA 98225-9080, USA*

[b] *Japan Marine Science and Technology Center, JAMSTEC, 2-15 Natsushima-Cho, Yokosuka 237, Japan*

Received 12 August 2002; received in revised form 7 November 2002; accepted 8 November 2002

Abstract

Drilling off of the Costa Rica margin during Ocean Drilling Program Leg 170 penetrated the complete sediment section seaward of the Middle Americas Trench (MAT) at one location (Site 1039), and sections through the margin wedge, décollement, and subducting sediments at two locations (Sites 1040 and 1043) near the toe of the wedge. Analyses of these sediments and their structures indicated that the margin wedge is not constructed by offscraping of the present incoming sediments, but is an older (perhaps accreted) structure. Nearly the entire section of sediments entering the MAT is thrust beneath the margin wedge. Anisotropy of magnetic susceptibility (AMS) and paleomagnetic data provide insight into the initial stages of fabric development associated with formation of the active décollement fault. Within the décollement zone, fabric development is localized to the upper few meters of the décollement, as indicated by higher AMS *P* values and by fabric orientations. Below the décollement, the uppermost 180 m of the underthrust hemipelagic sediment section is also deformed, as indicated by comparison of fabrics and their orientations between the seaward reference site and the sites that penetrated the décollement. AMS foliations become progressively more anisotropic, and the orientation of these fabrics, following reorientation of the cores using paleomagnetism, dip landward within the underthrust sediment package. These data indicate that deformation involves thinning of the incoming sediment package by compaction produced by distributed shearing of the upper portion of the sediment package. The fabric data suggest that the uppermost 180 m of the underthrust sediments are undergoing incipient underplating beneath the margin wedge.

Keywords: underplating; Costa Rica; AMS; accretionary prisms; ODP

1. Introduction

The interaction between subducting and overriding plates at convergent margins controls or influences a vast array of geologic processes. Such processes include examination of mass-

* Corresponding author. Tel.: +1-360-6506573; Fax: +1-360-6507302.
E-mail address: bernieh@cc.wwu.edu (B.A. Housen).

0012-821X/02/$ – see front matter
PII: S0012-821X(02)01076-2

transfer and geochemical processes controlled by the 'subduction factory' [1,2], generation of large earthquakes along convergent-margin plate boundaries, [3], and processes of continent growth [4]. The fate of sediments carried by the subducting plate into the subduction zone will influence these large-scale processes. Incoming sediments may be off-scraped and frontally accreted, partially or completely thrust beneath the overlying plate, or transferred from the subducting plate to the bottom of the overlying plate via underplating. In order to determine which of these processes influence the sediment budget at a convergent margin, detailed structural analyses of the incoming sediment, its interaction with the décollement and/or other important faults, and the deformation behavior of any sediment thrust beneath the décollement needs to be conducted. Drilling and seismic reflection surveys play crucial roles in characterizing sediment deformation and the fraction of oceanic sediments that reaches subduction zones [4]. Sediments reaching depths great enough to influence the chemistry of arc magmas are identified by trace element [2] or cosmogenic isotopic [1] compositions of arc lavas.

The deformation of sediments at convergent margins is the result of an often complex interplay between sediment physical properties, fluid flow, and tectonics (see Moore and Vrolijk [5] for a review). One important set of data concerning the variation in mineral fabrics (both degree of alignment and fabric orientations) comes from magnetic anisotropy, primarily anisotropy of magnetic susceptibility (AMS). For example, AMS results from ancient accretionary prism sediments (Neogene Miura Group, Japan) have shown that such fabrics can accurately depict structural variations associated with both soft-sediment deformation and subsequent tectonic fabrics developed during folding and faulting of these prism rocks [6]. Studies utilizing AMS of samples collected from the Nankai [7] and Barba-

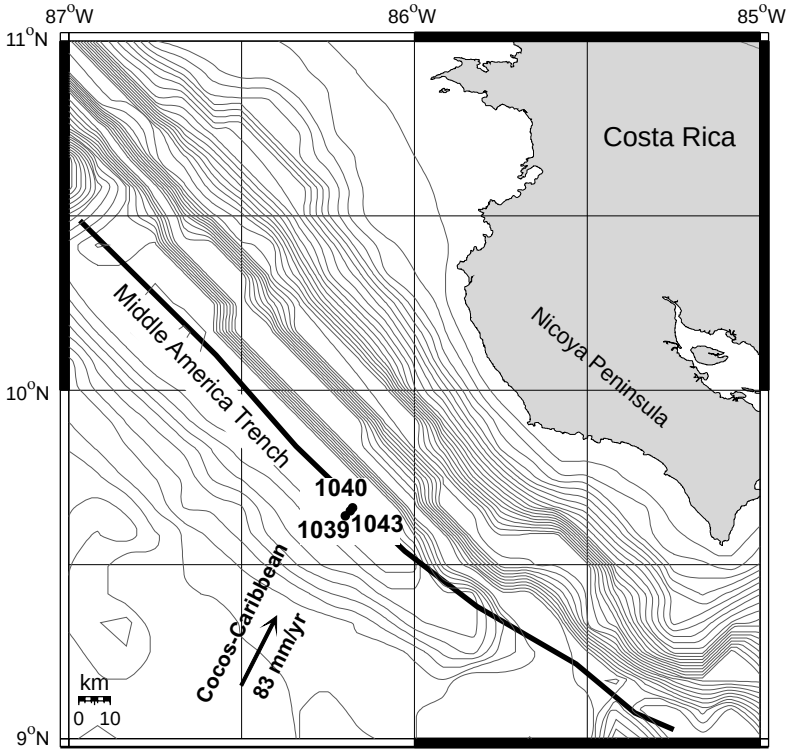

Fig. 1. Map of ODP Leg 170 area, showing location of Sites 1039, 1043, and 1040. For reference, the Cocos–Caribbean convergence vector [10] is shown.

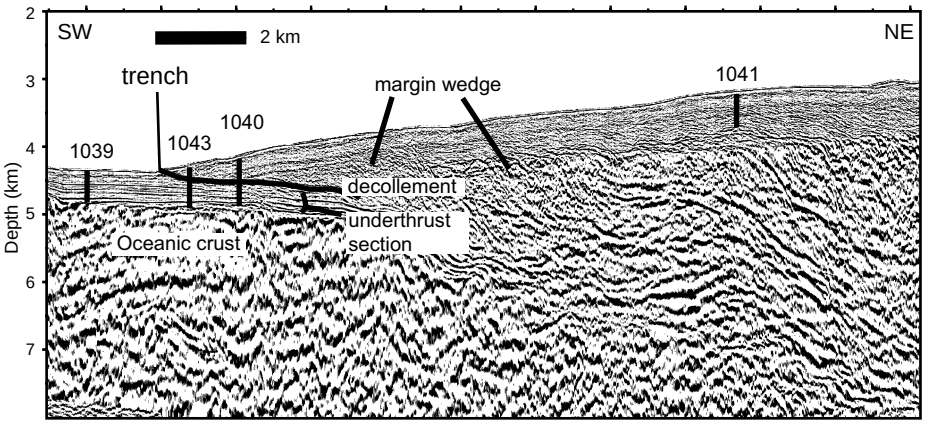

Fig. 2. Multichannel seismic reflection section (UTIG Line CR-20), modified from [14]. Locations of ODP Sites 1039, 1043, 1040, and 1041 are shown. The sediment section from the seafloor to the top of the oceanic crust was penetrated at Site 1039. This entire section is thrust beneath the margin wedge, as shown by drilling results at Sites 1043 and 1040.

dos [8] accretionary prisms clearly document strain variations within the frontally accreted prisms and their underlying décollement faults and underthrust sections. In this paper, we will present the first AMS results that document the deformation behavior of sediments that are thrust beneath a margin wedge that is non-accretionary (i.e. little or no frontal accretion of incoming material), illustrating deformation processes in sediments undergoing the initial stages of underplating.

2. Geology

During Ocean Drilling Program (ODP) Leg 170, cores were collected from five sites along a transect crossing the Middle Americas Trench (MAT) offshore of Costa Rica (Fig. 1) [9]. Here the Cocos plate is being subducted beneath the Caribbean plate, with a convergence rate of 83 mm/yr [10].

Site 1039 is located 1500 m seaward of the trench (Fig. 2). A total of section 448.7 m was drilled, recovering the entire sedimentary sequence as well as several meters of gabbro sills at the bottom of the hole. Site 1043 is located 600 m arcward of the trench (Fig. 2). A total of 482.3 m of section was drilled, recovering sediments from the prism, and the upper half of the underthrust sediment sequence. Site 1040 is located 1670 m arcward of the trench (Fig. 2). A total of 661.47 m of section was drilled, recovering prism sediments, the entire underthrust sediment sequence, as well as 11 m of gabbro sills at the bottom of the hole. The sediment sequences at sites 1039, 1043, and 1040 were divided into several lithostratigraphic units by the Leg 170 Science Party [9]. Of primary interest to this paper are the upper units at Site 1039 and their underthrust equivalents at 1043 and 1040 (Fig. 3). The uppermost unit, U1, occurs between 0 and 84.4 m depth and is composed of greenish-olive colored hemipelagic diatomaceous ooze with minor sand and silt layers. The next unit, U2, is composed of olive green colored hemipelagic silty clay and occurs from 84.4 to 152.5 m depth. Below these units, the sediments are composed of pelagic nannofossil chalks (unit U3). Studies of microfossils and magnetostratigraphy indicate the U1 and U2 sediments at Site 1039 are between 0 and 4 Ma [9].

Based on a number of lines of evidence, it is apparent that nearly the entire sediment section drilled at Site 1039 has been thrust beneath the Costa Rica margin wedge. Shipboard evidence collected during Leg 170 (lithostratigraphy, biostratigraphy, and magnetostratigraphy) indicate that all parts of sedimentary units U1, U2, and U3 can be identified in the underthrust sections drilled at Sites 1043 and 1040 [9]. Studies of cosmogenic isotopes, logging-while-drilling (LWD)

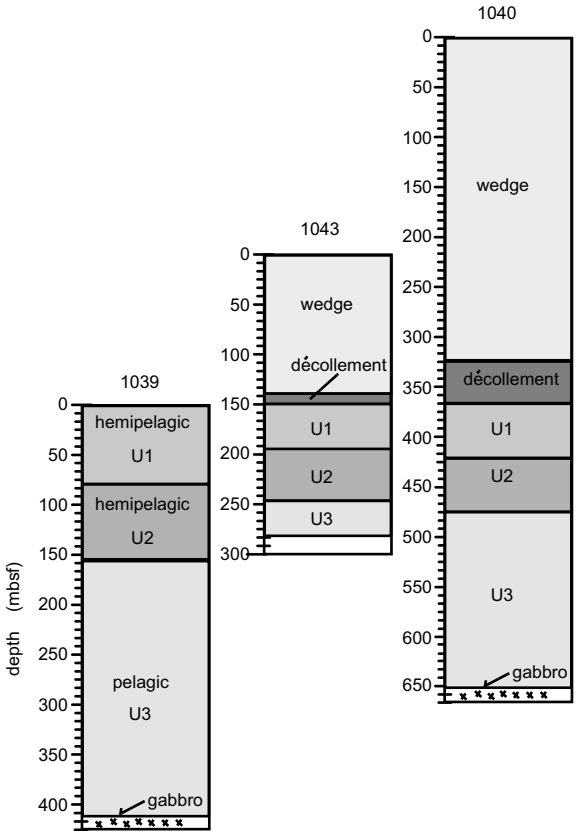

Fig. 3. Lithologic and structural variations of Sites 1039, 1043, and 1040. The depth range in meters below sea floor (mbsf) of the three sediment units, hemipelagic unit U1, hemipelagic unit U2, and pelagic unit U3 are indicated for all three sites. For Sites 1043 and 1040, the depth ranges of the margin wedge and décollement zone are also indicated.

results, and velocity analysis of multichannel seismic (MCS) reflection data subsequently confirmed these observations.

Morris et al. [11] measured the abundance of ^{10}Be in sediments from the wedge and underthrust section. Sediment units U1 and U2 from Site 1039 and their underthrust equivalents at Site 1040 have abundant cosmogenic ^{10}Be in the uppermost 100 m. Little or no cosmogenic ^{10}Be was found in the wedge, indicating its sediments were all >3–4 Ma in age and do not contain any portion of the hemipelagic sediments admixed by offscraping.

Saito and Goldberg [12] examined density, resistivity, and natural gamma-ray logs collected by LWD at Sites 1039 and 1043. Such LWD logs provide essentially continuous measures of these sediment physical properties through the drilled interval. This technique is a vast improvement in its ability to extract logging data from environments such as accretionary prisms where hole instability most often leads to incomplete core recovery and poor or non-existent wire-line logging data (see Moore et al. [13]). In general, the LWD results also confirm that the entire sediment sequence is thrust beneath the margin here by detailed correlations between logging data from Sites 1039 and 1043. The LWD density results also indicate that sediment layers in the upper hemipelagic section (units U1 and U2) at Site 1039 are less dense than their underthrust equivalents at Site 1043. This suggests that the upper section of Site 1043 has undergone between 20 and 40% volume reduction as a result of being thrust beneath the margin wedge [12].

McIntosh and Sen [14] obtained improved determination of true depths in the seismic data through the use of the LWD density logs, producing detailed estimates of fine-scale variations in sonic velocity in the Site 1039, 1043, and 1040 sections. Their analysis of the Leg 170 transect indicated that relative to unit thicknesses observed at Site 1039, the upper hemipelagic units were greatly thinned at Sites 1043 and 1040. Their analysis is also very valuable in that it can be applied to other portions of the extensive MCS data set collected at this margin. In some portions of this margin, the MCS data suggest that thinning of the hemipelagic section thrust under the Costa Rica margin wedge has resulted in underplating of these sediments.

Both the MCS [14] and LWD [12] data indicate that 20–40% volume loss has occurred in the upper hemipelagic section of the underthrust sediments. This volume loss is most likely nearly all in the form of porosity reduction, with attendant volumes of expelled pore fluid. The geologic cause of the porosity reduction is very likely rapid tectonic loading of the sediment section as it is thrust beneath the margin wedge. This process gives rise to significant volumes of expelled water, and can in many cases lead to excess ($>$lithostatic) pore fluid pressures [15]. An idea of how rapid this tectonic loading is relative to normal depositional

loading can be had by comparing the sedimentation rates of the hemipelagic section at Site 1039 with the rate at which these sediments are thrust beneath the margin wedge. Shipboard magnetostratigraphy and biostratigraphy [9] found that the upper 50 m of the hemipelagic section accumulated at a rate of 105 m/Ma. Given the plate convergence rate (83 km/Ma), distance from the trench to Sites 1043 (600 m) and 1040 (1670 m), and thickness of sediment in the wedge above each site (150 m at 1043 and 360 m at 1040), 'subduction loading rates' can be calculated. Values of 20.5 km/Ma (Site 1043) and 17.9 km/Ma (Site 1040) for the underthrust sediments are obtained. These rates indicate tectonic loading of sediments can be several orders of magnitude more rapid than depositional loading. By examining the mineral fabrics in these sediments, the geometry of this compaction strain can be inferred, which will lead to a better understanding of both the sediment dewatering process and the development of tectonic fabrics in sediments. Important questions that can be answered include: What is the dominant volume loss process (vertical compaction, or tectonic shortening) in the underthrust sediments (Saffer et al. [15])? Are matrix minerals aligned sufficiently to control permeability anisotropy? Is there any fabric evidence for incipient underplating? We will address these questions through measurement of magnetic anisotropy.

3. Samples and methods

A total of 1740 oriented samples were collected from Sites 1039, 1043, and 1040, with an average interval of 70 cm between each sample. The samples were enclosed in 10 cm^3 plastic cubes, collected from the cores by carefully cutting the sediment with a large (no. 22) surgical scalpel. Samples were collected from the interior of the core to avoid possible core deformation. Each sample was stored in a refrigerated enclosure to prevent the sediment from drying out. AMS was measured with either a KLY-2 Kappabridge (Ocean Research Institute, University of Tokyo), or a KLY-3S Kappabridge (Western Washington University). For 950 of the samples from the margin wedge and units U1 and U2, paleomagnetic measurements were made at WWU, using a 2-G 755 DC-SQUID magnetometer. Stepwise alternating-field demagnetization (using 5 mT steps from NRM to up to 190 mT) was employed to define the characteristic remanence direction, which was determined from the data using principal component analysis (PCA) [16]. The paleomagnetic data will be reported in a future contribution, and were used to reorient the rotary drill core for Sites 1039 and 1043 using the method described in [17]. This enables the cores to be restored to geographic coordinates, but the method has several important limitations. The most important is that any true vertical-axis rotation of portions of the drilled interval (which would be expected in cases of oblique convergence, and perhaps between thrust sheets) will not be resolvable by these data.

4. AMS results

4.1. Site 1039

For Site 1039, bulk magnetic susceptibilities largely reflect the variations in lithology. The upper hemipelagic units have generally high susceptibilities (5×10^{-4} to 4×10^{-3} SI volume units), and the lower pelagic nannofossil chalk unit has very low (5×10^{-5} to -6×10^{-6}) susceptibilities (Fig. 4). Based on these bulk susceptibilities, shipboard mineralogical analyses (visual and X-ray diffraction (XRD)) and thermal demagnetization of IRM [9], the carriers of susceptibility are detrital magnetite and paramagnetic clays in the hemipelagic section and an admixture of diamagnetic carbonates, magnetite, and minor paramagnetic clays in the pelagic section. The mixture of fabrics from diamagnetic minerals (with negative susceptibilities) and fabrics from para/ferrimagnetic minerals (with positive susceptibilities) in the pelagic section gives rise to composite AMS fabrics with very low susceptibility, spurious results with a positive k_{max} and a negative k_{min}, and attendant large errors in both orientation and in ellipsoid parameters such as degree of anisotropy. Because of this, no meaningful interpretation of the AMS fabrics in the majority of the pelagic section (unit

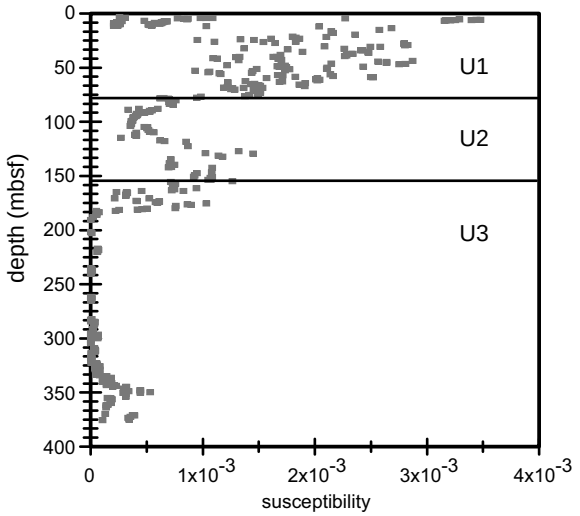

Fig. 4. Magnetic susceptibility, in SI volume units, as a function of depth for Site 1039 samples.

U3) of Site 1039 or Site 1040 can be made. Due to this mineralogical complexity, and because recovery of unit U3 at Site 1043 was incomplete, analyses of AMS fabrics from Site 1039 will be confined to the upper hemipelagic units U1 and U2. The AMS fabrics in these samples are very weak, with a degree of anisotropy ($P = k_{max}/k_{min}$) between 1.005 and 1.015 (Fig. 5). The orientations of the AMS fabrics are best characterized by the inclination of the k_{min} axes. For Site 1039, the k_{min} axes have inclinations scattered between 30° and 80° (Fig. 5). The weak fabrics indicate that the minerals in these sediments are very poorly aligned, which is reflected in the large scatter in the orientation of the AMS axes.

4.2. Site 1043

The Site 1043 results can be examined in two parts: those from the margin wedge and décollement, and the underthrust hemipelagic units. The wedge sediments have low magnetic susceptibility (1×10^{-4} to 5×10^{-4}), variable degrees of anisotropy (P between 1.02 and 1.06), and orientations of k_{min} that range from sub-vertical in the upper portion of the wedge to inclinations of around 30° near the base of the wedge (Fig. 6). The décollement occurs between 140 and 151 m depth and has somewhat higher anisotropy (P between 1.04 and 1.07), with k_{min} axes inclined at about 45° throughout the décollement interval (Fig. 6).

Compared to the fabrics in the same sediment sequence at Site 1039, the AMS data from the underthrust section at Site 1043 (Fig. 6) have slightly lower susceptibilities (5×10^{-4} to 1×10^{-3}) and slightly higher degrees of anisotropy

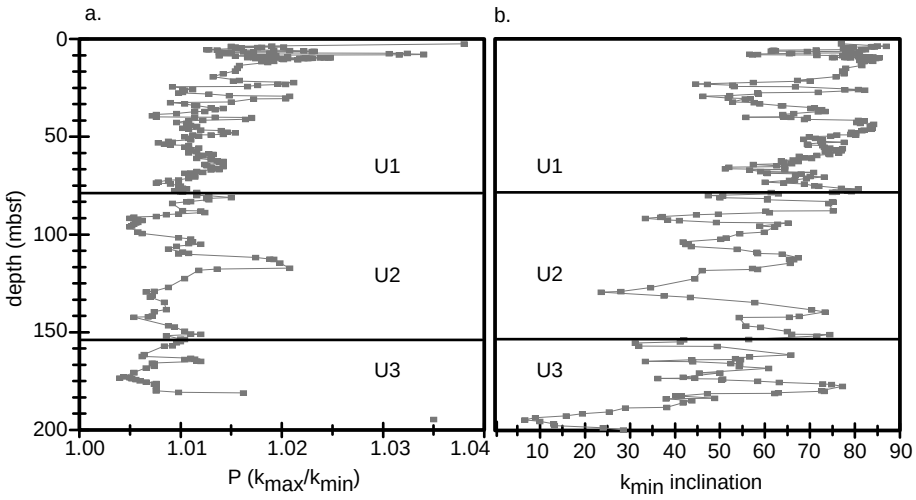

Fig. 5. Anisotropy of magnetic susceptibility (AMS) results for the uppermost 200 m of Site 1039. (a) Degree of anisotropy (P), and (b) the inclination (degrees) of the minimum susceptibility axis. The positions of lithologic units (U1, U2, and U3) within this interval are indicated.

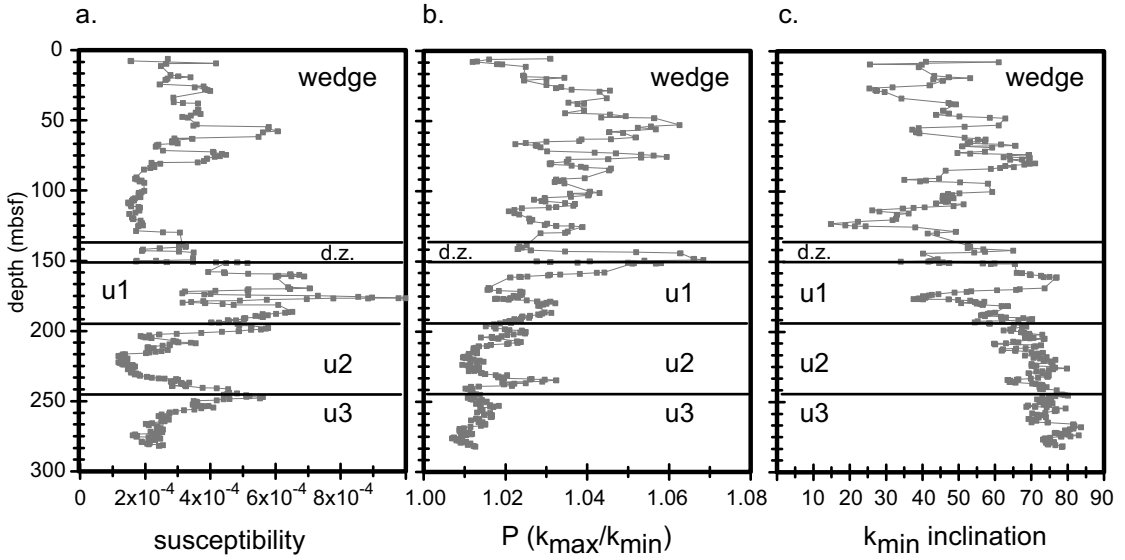

Fig. 6. AMS results for Site 1043 samples. (a) Magnetic susceptibility (SI volume units), (b) degree of anisotropy (P), and (c) inclination of the minimum susceptibility axis. The positions of lithologic units U1, U2, and U3, as well as the décollement zone and margin wedge, are also indicated.

(P between 1.01 and 1.03). The k_{min} axes become progressively more steeply inclined with depth (Fig. 6).

4.3. Site 1040

For Site 1040, the margin wedge sediments have high susceptibilities (5×10^{-4} to 1×10^{-3}) in the upper 25 m, low susceptibilities from 25 to 275 m, and high susceptibilities from 275 m to the base of the wedge sediments at 330 m (Fig. 7). The degree of anisotropy varies between 1.02 and 1.07 within the wedge, with orientations of k_{min} axes steeply inclined (40°–70°) in the upper portion of the wedge, with shallower (15°–40°) inclinations in the lower portion of the wedge (Fig. 7). At Site 1040, the décollement occurs between 330 and 368 m depth. At the top of this interval, the AMS axes have shallow inclinations (15°–30°), and for the most part low (P between 1.03 and 1.06) degrees of anisotropy.

The underthrust sediments at this site have AMS results that are very similar to those of Site 1043. The susceptibility is high (5×10^{-4} to 3×10^{-3}), the degree of anisotropy decreases throughout the hemipelagic interval (from $P=1.06$ at the top to $P=1.02$ at the base of the sequence), and the orientation of k_{min} axes is steep, varying from 45° to 85° (Fig. 7).

5. Discussion

The AMS results reported above provide a measure of the orientation and degree of alignment of matrix clays and accessory magnetite. It is important to note that these fabrics record the bulk-preferred orientation of these minerals for the entire sample's volume. Other structures, most notably brittle fractures and volumetrically small structures with internal mineral fabrics (such as deformation bands), will not be effectively measured by techniques such as AMS. As such, AMS results should be viewed as representative of the orientation and shape of the strain ellipsoid in weakly deformed sediments such as these (see Borradaile [18] for a review). It is also important to note that significant changes in mineralogy can influence the interpretation of AMS results, so that it is important to confine discussion of changes in fabrics within a set of variably deformed rocks or sediments to results that come

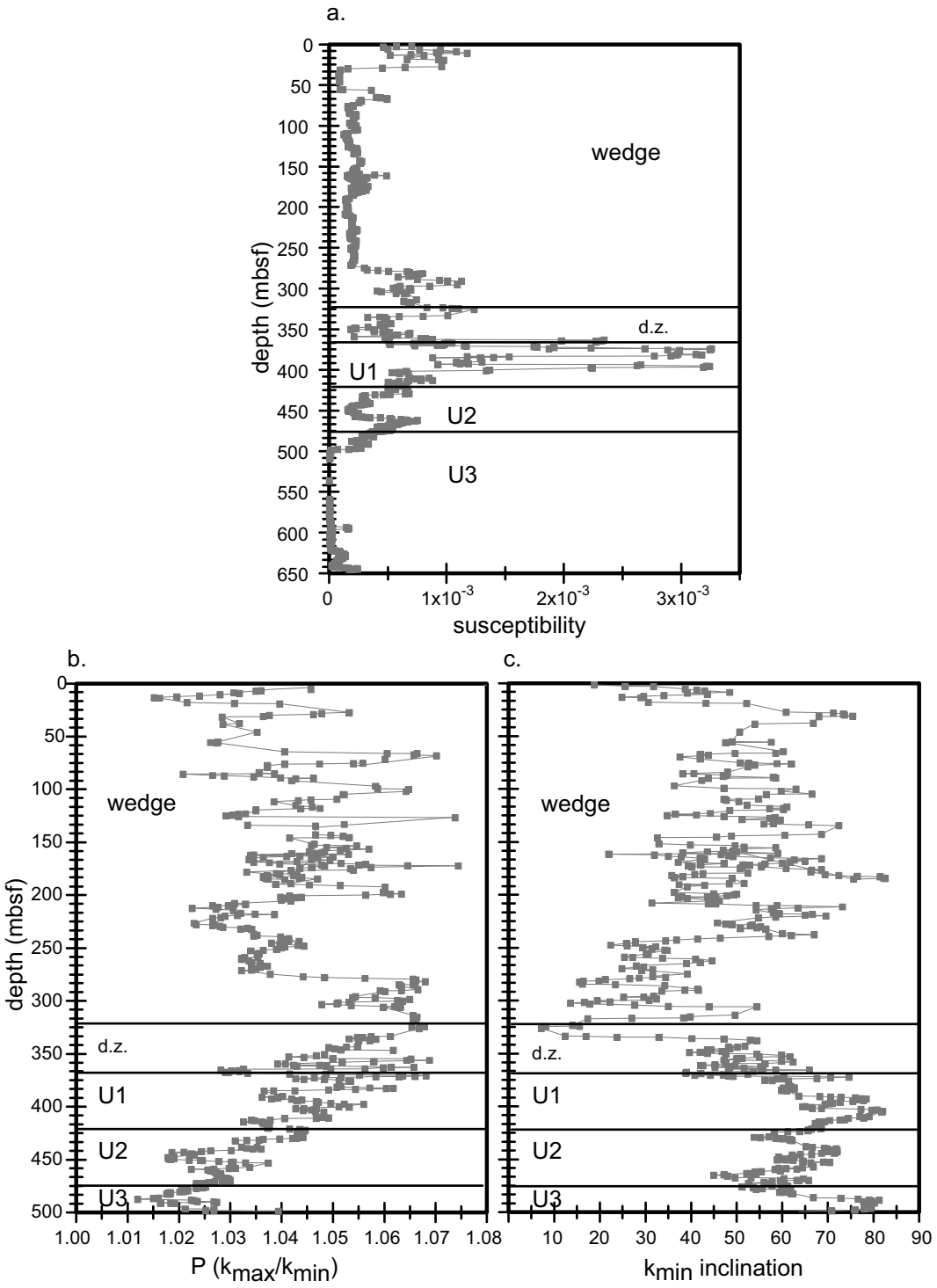

Fig. 7. AMS results for Site 1040 samples. (a) Magnetic susceptibility (SI volume units), (b) degree of anisotropy (P), and (c) inclination of the minimum susceptibility axis. Note change in depth scale for panels b and c. The positions of lithologic units U1, U2, and U3, as well as the décollement zone and margin wedge, are also indicated.

from similar lithologies. Here, we can use the essentially identical sediment section containing hemipelagic units U1 and U2 found at Sites 1039, 1043, and 1040 for this fabric comparison. In addition, the orientation and shape of the AMS ellipsoid at Site 1039 provides information on the pre-existing depositional/compaction fabric present in the sediments prior to underthrusting. Thus changes in the AMS fabrics at Sites 1043 and 1040 relative to these initial fabrics can be used to evaluate the progression of deformation. Of importance to this discussion, the orientation of k_{min} can serve as an indicator of the shortening direction in these sediments. Comparing AMS results with analyses of small-scale and brittle structures can provide complementary information about strain partitioning in deformed sediments.

Vannucchi and Tobin [19] examined small-scale structures found in cores from Sites 1043 and 1040. They found an array of structures, ranging from relatively isolated fractures to networks of deformation and shear bands within the margin wedge sediments. In general, they found an increase in the number and spatial density of structures such as deformation bands in the lowermost portion of the margin wedge at Sites 1043 and 1040, immediately above the top of the décollement zone at these sites. On the basis of kinematic analyses of brittle structures, they concluded that these structures formed during episodic pulses of high-pressure fluids. The state of stress and its resulting strain varied from gravitational-loading-dominant stress at the top of the wedge, to an increasing contribution from sub-horizontal tectonic shortening in the sediment at the base of the wedge [19]. The AMS results from the wedge sediments agree very well with the structural analysis of Vannucchi and Tobin [19]. The trend of k_{min} orientations shown in Figs. 6 and 7 indicates that k_{min} inclinations become progressively shallower as the base of the margin wedge is approached at Sites 1043 and 1040. This indicates a change from steeply inclined (gravitationally controlled) shortening in the upper portion of the wedge, to shallowly inclined (tectonically controlled) shortening near the base of the wedge.

Within the décollement, AMS fabric interpretation is complicated by two factors. First of all, due to the limited extent of the décollement and incomplete recovery of sediments in cores from this interval, the number of samples available for AMS analyses is small. Secondly, the lower portion of the décollement at both Sites 1043 and 1040 is composed of very dense sticky clay, which was severely deformed by continuous and penetrative rotary shearing during the drilling process [9]. Intervals of core deformed in this manner were clearly recognized by spiraling sediment features and continuous azimuthal rotation of shipboard remanence directions, and were not sampled for this study. That having been said, we can make some interesting observations using matrix fabrics within the décollement. The AMS results from the uppermost portion of the décollement at Sites 1043 and 1040 have relatively low anisotropy degrees (P between 1.02 and 1.04). The development of relatively weak fabrics within these faults indicates little ductile alignment of matrix minerals has occurred and that brittle structures accommodate the majority of strain. This is similar to the behavior of other décollements for which AMS data are available. Both the Barbados [8] and Nankai [7] décollement zones are marked by very weak magnetic anisotropy, indicating that matrix mineral fabrics are poorly developed. At Barbados and Nankai, strain orientations abruptly change across the uppermost portion of these two décollements as well, indicating that strains are efficiently decoupled and that these faults are very weak in relation to the surrounding sediments. In contrast, the décollement zone at the Costa Rica margin appears to have a more gradual change in fabric orientation (see Figs. 6c and 7c) that coincides with slightly higher degrees of anisotropy within the uppermost few meters of the fault zone. These observations suggest that the fault zone here accommodates more ductile deformation than either the Barbados or Nankai décollements. The Costa Rica décollement may be, relative to the surrounding sediments, somewhat stronger than the Barbados or Nankai examples. Ultimately it may be possible to utilize the spatial variation of fault zone fabrics, in conjunction with relevant kinematic information, to address questions of fault zone strength in a more absolute sense (e.g. [20]).

At this point, such interpretations are complicated by the interaction between pure and simple shear, sediment volume loss, and incomplete recovery of samples from this fault zones (see further discussion below).

The underthrust sediments provide a wealth of interesting observations. First of all, analyses of small-scale structures [9,19] indicate that the underthrust units at Site 1043 and 1040 are little deformed. Minor faulting and thin (2–4 cm) intervals of deformation bands were found within the hemipelagic units U1 and U2 at both sites [19]. Aside from these structures, only minor compaction-related mineral alignment was mentioned. On a larger scale, some bedding tilt was observed within the upper hemipelagic sequence [9,19]. The AMS results from the underthrust sequence at both Sites 1043 and 1040 have k_{min} orientations that progress from moderately to steeply inclined as a function of depth. Along with this change in fabric orientation, the degree of anisotropy becomes smaller as a function of depth as well (Figs. 6 and 7). If the hemipelagic sediment in the underthrust sequence were simply being sub-

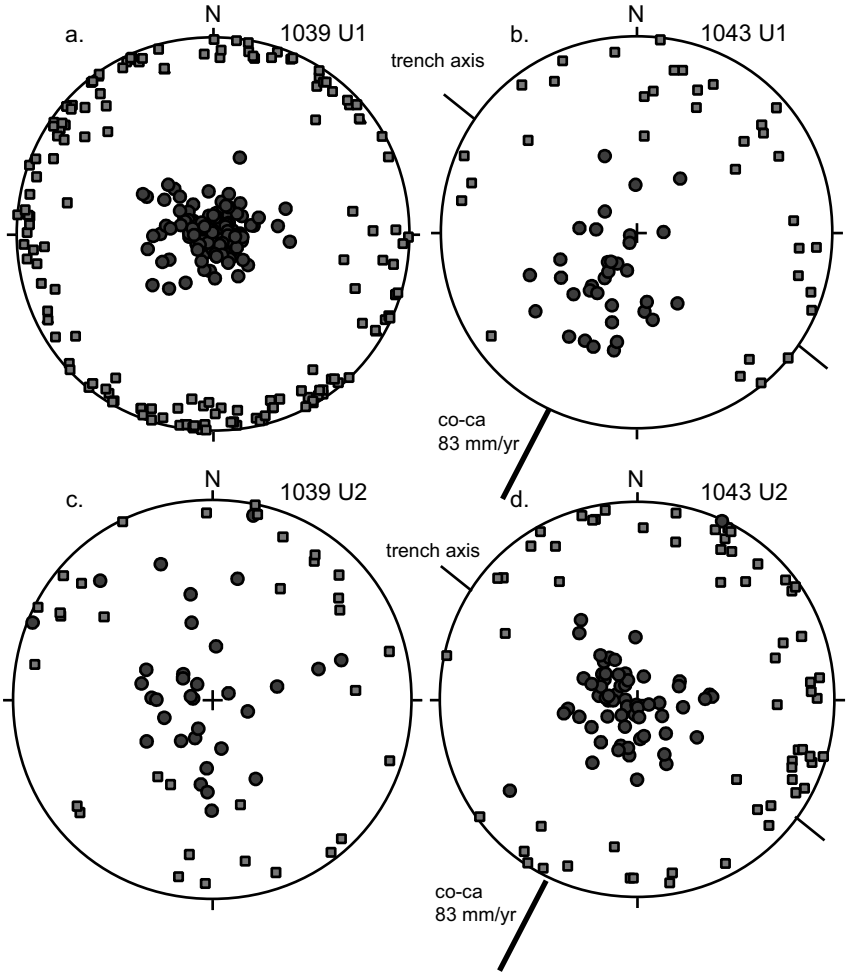

Fig. 8. Orientations of AMS axes, corrected for core rotation using paleomagnetic data. Maximum susceptibility axes plotted as squares, intermediate susceptibility axes plotted as triangles, and minimum susceptibility axes plotted as circles. (a) Site 1039, unit U1. (b) Site 1043, unit U1. (c) Site 1039, unit U2. (d) Site 1043, unit U2. For reference, the Cocos–Caribbean convergence vector and strike of the Middle America Trench axis are plotted for the Site 1043 data. AMS orientations from Site 1043, unit U1 define a planar fabric, with the flattening plane dipping towards the NE.

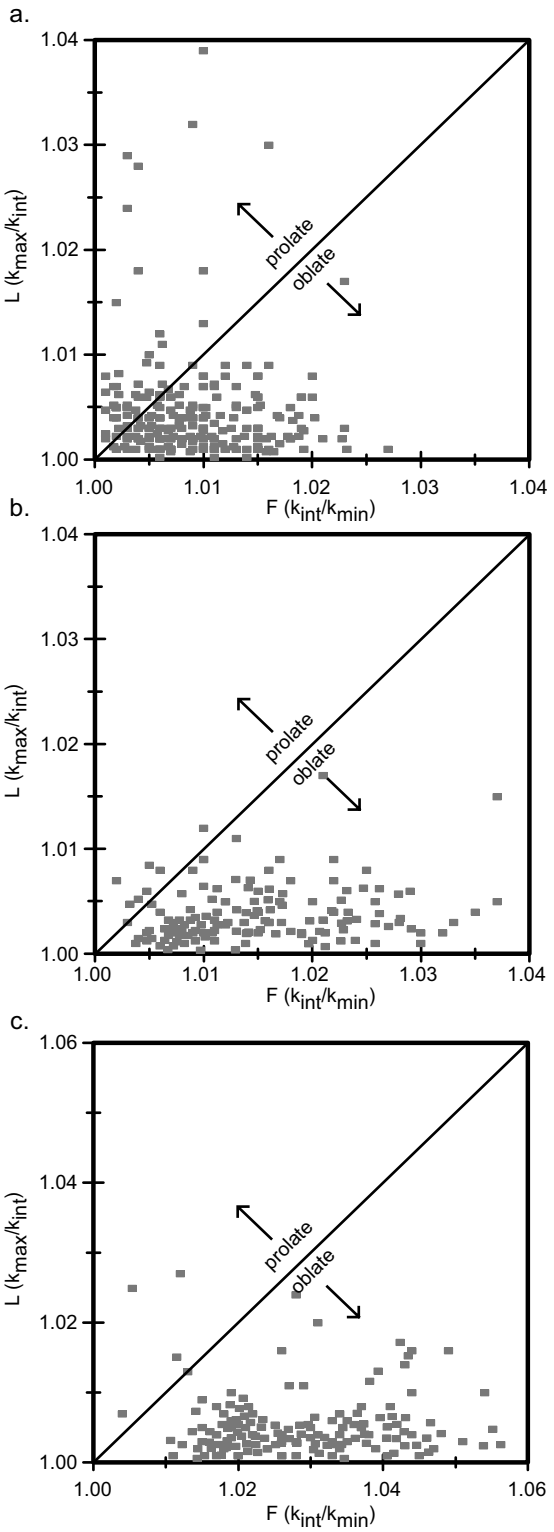

jected to gravitational loading by the overlying margin wedge, one would expect to find sub-vertical k_{min} orientations, as is the case in underthrust sediments at both the Nankai and Barbados prisms [7,8]. The degree of anisotropy will reflect the relative degree of compaction. For the case of simple compaction of a uniformly drained section, P values should increase with depth. For a section of sediments that undergoes drainage for the top [21], greater compaction would occur at the top of the section, producing a pattern of initially high P values at shallower depths, with a decrease in P values expected at greater depths. The inclined k_{min} orientations, and to a lesser extent the relatively more intense AMS fabrics, indicate that the underthrust hemipelagic sequence is being deformed by a significant component of tectonic strain. This agrees with prior structural observations [9,19]. The tectonic nature of the AMS fabrics in the underthrust hemipelagic units can be further demonstrated by examining the AMS axes after reorientation using the paleomagnetic results. The reoriented AMS data from the reference site (1039) have k_{min} that are clustered, within error, about vertical, and the k_{max} orientations all have sub-horizontal inclinations but do not have any azimuthal clustering (Fig. 8). The few exceptions, from Site 1039 unit U2, with shallow k_{min} orientations may be due to either very weak fabrics with large error, or to inverse AMS fabrics (from carbonates or SD magnetite). For the underthrust unit U1 at Site 1043, the k_{min} orientations are streaked out along a great circle trending NE–SW (Fig. 8). The k_{max} orientations are concentrated in two weakly defined groups, one sub-horizontal and trending NW–SE and the other shallowly plunging toward the NE (Fig. 8). The NE–SW streaking of the k_{min} orientations is parallel to the Cocos–Caribbean convergence vector [10], with the AMS foliations in unit U1 being tilted toward the arc. Hemipelagic unit U2 has AMS orientations that have steeply inclined k_{min}, and k_{max} orientations that are not

←

Fig. 9. Flinn-type plots, showing the shape of the AMS ellipsoid for hemipelagic units U1 and U2 at (a) Site 1039, (b) Site 1043, and (c) Site 1040.

well clustered as seen in unit U1 (Fig. 8). These AMS orientations suggest that gravitational loading deforms the lower hemipelagic sequence (U2) at Site 1043.

Comparing the AMS ellipsoid shapes for the hemipelagic sediments from Sites 1039, 1043, and 1040 also provides interesting insights into the style of their deformation. Ellipsoid shapes are depicted best on standard Flinn plots. For Site 1039, the AMS ellipsoid shapes are nearly isotropic, with a very slight trend toward oblate shapes (Fig. 9). The AMS ellipsoids of hemipelagic sediments in the underthrust section at Sites 1043 and 1040 are uniaxial oblate, with the Site 1040 ellipsoids being more anisotropic (Fig. 9). Because the hemipelagic sediments are all of the same composition at all three sites, the differences in their AMS ellipsoid shapes provides a measure of the nature of the progression of deformation during the early stages of rapid tectonic loading as the section is dragged beneath the margin wedge. The uniaxial-oblate AMS fabrics indicate that compaction may have occurred as true flattening, with the shortening direction given by the orientation of the k_{min} axes. Consideration of volume loss in the underthrust sediments complicates this interpretation. Based on core physical properties and the LWD density data from both Sites 1043 and 1040, unit U1 has undergone 30–40% volume reduction and unit U2 has undergone 20% volume reduction relative to the same material at Site 1039 [9,12]. Volume loss will shift the $k = 1$ (plane strain) line on the Flinn-type plot towards the right. This would produce an apparent flattening ellipsoid by combination of a plane strain (such as shear strain) and volume loss. It is clear, however, that AMS fabrics become increasingly more anisotropic with increasing depth of underthrusting (Fig. 10). Thus, the AMS data are recording the loss of volume (in the form of porosity reduction) by increasing alignment of minerals within these sediments.

There are several possible explanations for the pattern of fabric orientation and anisotropy we have found in the upper portion of the underthrust sequence. The rotation of fabrics within this interval indicates that simple shear (with volume loss and/or a component of pure shear) is a

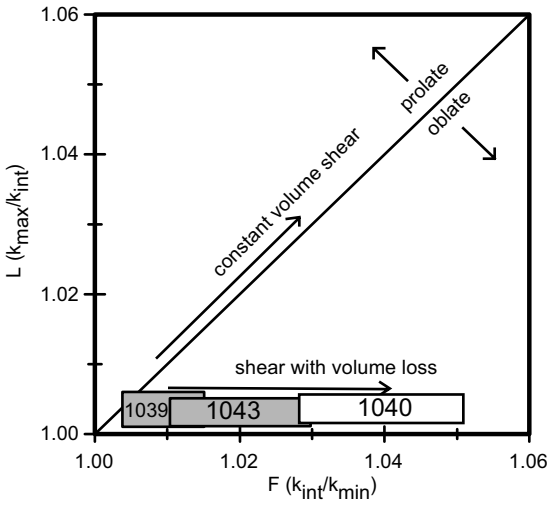

Fig. 10. Flinn-type plot, showing progressive deformation of the hemipelagic sediments. The boxes represent region of the Flinn diagram enclosed by the mean and standard deviation of the L and F values for all samples from units U1 and U2 at each site. The AMS results show a clear progression from weakly anisotropic fabrics at Site 1039, to progressively more anisotropic and uniaxial-oblate fabrics at Sites 1043 and 1040. Arrows denoting two possible paths of progressive strain fabrics, one denoting constant-volume simple shear, and the other denoting simple shear with volume loss, are indicated for reference.

significant component of the strain (and resultant fluid expulsion) in these sediments. Thinning of the upper hemipelagic units and progressive change in the orientation of k_{min} axes from moderately inclined in unit U1 to nearly sub-vertical in unit U2 at Sites 1043 and 1040 is consistent with the interpretation of MCS data made by McIntosh and Sen [14] that these units are being underplated beneath the margin wedge (Fig. 11). In this case, the AMS fabrics reflect deformation associated with an incipient stage of underplating. This structural geometry is also similar to that observed in underplated sediment packages in ancient melange units now exposed on land, such as the Shimanto Belt [22].

Another possible alternative is that these fabrics represent thickening of the Costa Rica décollement zone, most likely via a strain-hardening process [23]. The pattern of simple shear combined with increasing fabric intensity would be consistent with this process and agrees with shipboard

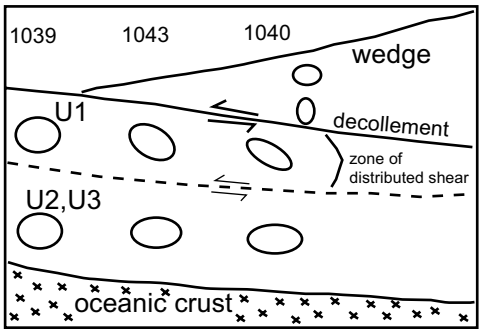

Fig. 11. Cartoon illustrating differences in deformation behavior at different locations within the Costa Rica margin. The ovals denote relative strains, with the orientation of the principal shortening direction denoted by the short axis of each oval. Seaward of the trench (Site 1039), fabrics are weak, indicating modest compaction of the sediment sequence. Rapid loading of the underthrust sediments beneath the margin wedge produces vertical compaction in underthrust units U2 and U3. A combination of simple shear (as required by the rotation of fabrics) and volume loss (due to both gravitational loading by the wedge and to the shear strain) occurs within hemipelagic unit U1. This unit is progressively thinned beneath the wedge [14], and the marked change in AMS orientations between units U1 and U2 (see Fig. 9) may suggest that an incipient fault zone is developing near the unit U1–U2 contact. Within the margin wedge, shortening is sub-vertical in the upper portion, and becomes more sub-horizontal near the top of the décollement zone.

observations that the décollement zone at Site 1040 is thicker than that at Site 1043 [9]. The deformation of the uppermost 50–100 m of the incoming hemipelagic sequence does indicate that the décollement separating the overlying margin wedge from the underthrust sequence allows some significant degree of structural coupling across the décollement. In an incipient state, structures produced by either underplating or by shear zone thickening would be very similar.

6. Conclusions

We have found that AMS fabrics from a transect of holes drilled through the Costa Rica margin provide a wealth of information regarding the initial stages of deformation of underthrust sediments in a non-accretionary prism. By comparing AMS results from undeformed hemipelagic sediments at a reference site seaward of the deformation front (Site 1039), with deformed versions of this same hemipelagic sequence that have been thrust beneath the margin wedge (Sites 1043 and 1040), the progression of deformation style can be accurately tracked in this deformation environment. Our primary conclusion is that a sequence of fabric rotation and increasing degree of anisotropy and of more oblate AMS ellipsoid shapes reflects a combination of simple shear, a possible contribution by pure shear, and volume loss in the hemipelagic sequence (Fig. 11). The sequence of deformation that we have documented is consistent with a process of incipient underplating, and could serve to confirm other structural interpretations of the Costa Rica margin calling for underplating of the upper hemipelagic sequence [14]. Incipient underplating is difficult to distinguish from a fault zone thickening process, especially where core recovery is incomplete. Both underplating or fault zone thickening would, however, serve to transfer material from the sediment section moving towards deeper portions of the subduction zone to the deforming wedge/décollement section that is properly part of the overriding plate. Underplating of these younger sediments before they reach significant depths within the subduction zone is consistent with the lack of cosmogenic ^{10}Be in Costa Rica arc magmas [11]. The scale of this underplating process beneath deeper portions of the margin wedge cannot be resolved by this study. In fact, other evidence [24] indicates that the margin wedge here has undergone net subsidence, which would indicate that underplating is either not occurring on a volumetrically large scale, or that other processes such as subduction erosion counterbalance any underplating that does occur.

Acknowledgements

Tammy Fawcett, Elizabeth Kilanowski, and Allison Dean are thanked for their assistance in measuring the AMS and paleomagnetism of these samples. Discussions with Harold Tobin, Paola Vannucchi, and our colleagues who sailed with us on ODP Leg 170 have improved this work. Very helpful comments by reviewers Demian

Saffer and Mark Hounslow also helped to improve this manuscript. Support for this project from JOI-USSSP and NSF OCE-9796173 is acknowledged. The cryogenic magnetometer at WWU was obtained with funds from NSF EAR-9727032.*[RV]*

References

[1] J.D. Morris, W.P. Leeman, F. Tera, The subducted component in island arc lavas: Constraints from Be isotopes and B-Be systematics, Nature 344 (1990) 31–36.
[2] T. Plank, C.H. Langmuir, Tracing trace elements from sediment input to volcanic output at subduction zones, Nature 362 (1993) 739–742.
[3] D.K. Rea, L.J. Ruff, Composition and mass flux of sediment entering the world's subduction zones: Implications for global sediment budgets, great earthquakes, and volcanism, Earth Planet Sci. Lett. 140 (1996) 1–12.
[4] R. von Huene, D.W. Scholl, Observations at convergent margins concerning sediment subduction, sediment erosion, and the growth of continental crust, Rev. Geophys. 29 (1991) 279–316.
[5] J.C. Moore, P. Vrolijk, Fluids in accretionary prisms, Rev. Geophys. 30 (1992) 113–135.
[6] T. Kanamatsu, E. Herrero-Bervera, A. Taira, Magnetic fabrics of soft-sediment folded strata within a neogene accretionary complex, the Miura Group, central Japan, Earth Planet. Sci. Lett. 187 (2001) 333–343.
[7] W.H. Owens, Magnetic fabric studies of samples from Hole 808C, Nankai Trough, Proc. ODP Sci. Results 131 (1993) 301–310.
[8] B.A. Housen et al., Strain decoupling across the décollement of the Barbados accretionary prism, Geology 24 (1996) 127–130.
[9] G. Kimura, E. Silver, P. Blum, et al., ODP Initial Reports 170, Texas A&M University, Ocean Drilling Program, College Station, TX, 1997.
[10] C. DeMets, R.G. Gordon, D.F. Argus, S. Stein, Effect of recent revisions to the geomagnetic reversal timescale on estimates of current plate motion, Geophys. Res. Lett. 21 (1994) 2191–2194.
[11] J. Morris, R. Valentine, T. Harrison, ^{10}Be imaging of sediment accretion and subduction along the northeast Japan and Costa Rica convergent margins, Geology 30 (2002) 59–62.
[12] S. Saito, D. Goldberg, Compaction and dewatering processes of the oceanic sediments in the Costa Rica and Barbados subduction zones: estimates from in situ physical property measurements, Earth Planet. Sci. Lett. 191 (2001) 283–293.
[13] J.C. Moore et al., Abnormal fluid pressures and fault-zone dilation in the Barbados accretionary prism: Evidence from logging while drilling, Geology 23 (1995) 605–608.
[14] K.D. McIntosh, M.K. Sen, Geophysical evidence for dewatering and deformation processes in the ODP Leg 170 area offshore Costa Rica, Earth Planet. Sci. Lett. 178 (2000) 125–138.
[15] D.M. Saffer, E.A. Silver, A.T. Fisher, H. Tobin, K. Moran, Inferred pore pressures at the Costa Rica subduction zone: implications for dewatering processes, Earth Planet. Sci. Lett. 177 (2000) 193–207.
[16] J.L. Kirschvink, The least-squares line and plane and the analysis of paleomagnetic data, Geophys. J. R. Astron. Soc. 62 (1980) 699–718.
[17] A. Taira, I. Hill, J.V. Firth, et al., ODP Initial Reports 131, Texas A&M University, Ocean Drilling Program, College Station, TX, 1991.
[18] G.J. Borradaile, Correlation of strain with anisotropy of magnetic susceptibility (AMS), Pure Appl. Geophys. 135 (1991) 15–29.
[19] P. Vannucchi, H. Tobin, Deformation structures and implications for fluid flow at the Costa Rica convergent margin, ODP Sites 1040 and 1043, Leg 170, J. Struct. Geol. 22 (2000) 1087–1103.
[20] R. McCaffrey, Oblique plate convergence, slip vectors, and forearc deformation, J. Geophys. Res. 97 (1992) 8905–8915.
[21] R. von Huene, H. Lee, The possible significance of pore fluid pressures in subduction zones, in: J.S. Watkins and C.L. Drake (Eds.), Studies in Continental Geology, AAPG Memoir 34, 1982, pp. 781–791.
[22] Y. Hashimoto, G. Kimura, Underplating process from melange formation to duplexing: Example from the Cretaceous Shimanto Belt, Kii Peninsula, southwest Japan, Tectonics 18 (1999) 92–107.
[23] J.C. Moore, T. Byrne, Thickening of fault zones; a mechanism for melange formation in accreting sediments, Geology 15 (1987) 1040–1043.
[24] P. Vannucchi et al., Tectonic erosion and consequent collapse of the Pacific margin of Costa Rica; combined implications from ODP Leg 170, seismic offshore data, and regional geology of the Nicoya Peninsula, Tectonics 20 (2001) 649–668.